ISSN 0915-633X

NATIONAL INSTITUTE FOR FUSION SCIENCE

Spatial Structure of Particle-Orbit Loss Regions in $l = 2$ Helical Systems

H. Sanuki, J. Todoroki and T. Kamimura

(Received – Nov. 2, 1989)

NIFS-9 Feb. 1990

RESEARCH REPORT
NIFS Series

NAGOYA, JAPAN

Spatial Structure of Particle-Orbit Loss Regions in $l = 2$ Helical Systems

H. Sanuki, J. Todoroki and T. Kamimura

National Institute for Fusion Science

Furocho, Chikusaku, Nagoya 464-01

ABSTRACT

Particle orbits and loss regions in both configuration and velocity space are studied on the basis of adiabatic invariants and guiding center drift equations. The boundary of loss region is determined from the condition whether the drift surfaces for both localized particles and transition particles between localized and blocked particles hit the limiter or not. Analytical form of loss region boundary for localized particle with $v_{\parallel} = 0$ is obtained. Effects of ripple modulation and electrostatic potential on particle confinement are also discussed.

Keywords : Helical system,orbit-loss, adiabatic invariant, drift equations

I. INTRODUCTION

A good understanding of particle orbits is very important for predicting the plasma confinement, high energy particle loss, and heating efficiency in a helical system. Particle orbits in these systems depend generally on many parameters such as aspect ratio, toroidal and helical ripples, particle energy, pitch angle, plasma potential, etc. To study particle orbits, several techniques of orbit calculations have been discussed. A typical method is to study the particle trajectries of many particles on the basis of guiding center drift equations. Another method is to use the adiabatic invariants. The former requires generally vast computations more than the latter.

In an asymmetric magnetic configuration under consideration, the momentum of charged particle is not conserved exactly. However, a constant of motion associated with a extended canonical momentum has been proposed [1] and applied to study the velocity space loss regions in existing machines [2]. Recently, Cary et al.[3] and Todoroki [4] discussed a more precise theory of adiabatic invariants. In this paper we analyze particle orbits and loss regions by using these adiabatic invariants. An analysis based on guiding center drift equations is also carried out.

In Section 2, the model of calculation is represented. The analytical scheme of loss region is explained in Section 3. Loss regions in configuration space are studied for several device parameters in Section 4. Effects of ripple modulation and electrostatic potential are also discussed in this section in connection with the reduction of particle loss. A numerical cal-

culation based on guiding center drift equations is carried out in Section 5. The last section is devoted to the conclusions.

II. MODEL OF CALCULATION

We apply the J - invariant method [3,4] to analyze particle orbits and to study a detailed spatial strusture of particle orbit loss regions in helical systems. For the analytic form of the adiabatic invariants it is necessary to specify a form for the magnetic field strength and electrostatic potential as functions of the coordinates. Here, the magnetic field strength and electrostatic potential are assumed to have the forms

$$B(\psi,\theta,\varphi) = B_0(\psi,\theta) - B_1(\psi,\theta)\cos(l\theta + M\varphi), \tag{1}$$

$$\Phi(\psi,\theta,\varphi) = \Phi_0(\psi), \tag{2}$$

with

$$B_0(\psi,\theta) = \overline{B}_0\varepsilon_0(\psi,\theta) \ , \tag{3}$$

$$B_1(\psi,\theta) = \overline{B}_0\varepsilon_1(\psi,\theta) \ . \tag{4}$$

The adiabatic invariants for this kind of stellarator configuration are given by [3,4]

$$J_{\tilde{\sigma}} = \tilde{\sigma}q\psi_p + 4B_\varphi\sqrt{\frac{m\mu}{B_1}}\left[(1+\gamma k^2)\Pi(\gamma,\frac{1}{k^2}) - K(\frac{1}{k^2})\right] / k, \quad (k>1) \tag{5}$$

$$J_r = 8B_\varphi\sqrt{\frac{m\mu}{B_1}}\left[(1+\gamma k^2)\Pi(\gamma k^2, k^2) - K(k^2)\right], \quad (k<1) \tag{6}$$

$$J_r = 8B_\varphi\sqrt{\frac{m\mu}{B_1}}\ \gamma^{1/2}\tan^{-1}\gamma^{1/2}, \quad (k=1) \ , \tag{7}$$

where ψ_p is the poloidal flux, we choose $B_\varphi = R_0\overline{B}_0$ to be constant, μ is the magnetic moment, q is the particle charge, m is the particle mass, and $\tilde{\sigma} = \pm$. In Eqs.(5) ~ (7), $\tilde{\sigma} = \pm$ and r indicate the species of a relevant

particle ($\tilde{\sigma}$ = +, positive passing, $\tilde{\sigma}$ = - , negative passing ; r , trapped) , K is the complete elliptic integral of the first kind and Π is the complete elliptic integral of the third kind ;

$$\Pi\ (\nu\ ;\ k^2) = \int_0^{\frac{\pi}{2}} \frac{d\varphi}{(1 + \nu\sin^2\varphi)(1 - k^2\sin^2\varphi)^{1/2}} .$$

Also, we defined the following two parameters for the derivation of Eqs.(5) ~ (7) ;

$$k^2 = [E - \mu B_0 + \mu B_1 - q\Phi_E] / 2\mu B_1 , \tag{8}$$

$$\gamma = 2B_1 / (B_0 - B_1) , \tag{9}$$

where E is the total energy, and $k > 1$ corresponds to passing particles and $0 \le k \le 1$ to trapped particles. If the limit $\gamma \to 0$ is taken, the adiabatic invariants (5) and (6) reduce to the conventional expressions

$$J_{\tilde{\sigma}} = \tilde{\sigma} q\psi_p + 8\frac{B_\varphi}{B_0}\sqrt{m\mu B_1}\, kE\ (\frac{1}{k^2}) , \tag{10}$$

$$J_r = 16\frac{B_\varphi}{B_0}\sqrt{m\mu B_1}\ [E(k^2) - (1 - k^2)K(k^2)] . \tag{11}$$

Since the finiteness of γ may have an influence upon particle drift orbits and loss regions in the systems with large M number or large helical ripple where γ becomes small but finite, particularly at the edge region of devices, the invariant forms (5) ~ (7) should be applied for particle orbit studies in these systems. In the following calculations, therefore, we use the invariant forms (5) ~ (7) .

We define the normalized minor radius ρ for labeling a flux surface

$$\rho = (\psi / \psi_e)^{1/2} , \tag{12}$$

where ψ_e is the value of ψ at the plasma edge. Magnetic field and potential are specified in the following forms ;

$$\varepsilon_0(\psi,\theta) = 1 + \varepsilon_a\rho\cos\theta , \tag{13}$$

$$\varepsilon_l(\psi,\theta) = \Big[\{\varepsilon_h + (\delta_h^{(-1)} + \delta_h^{(+1)}\rho^2)\varepsilon_a\rho\cos\theta\}^2 + \{(\delta_h^{(-1)} - \delta_h^{(+1)}\rho^2)\varepsilon_a\rho\sin\theta\}^2\Big]^{\frac{1}{2}} , \tag{14}$$

$$\Phi_E(\psi,\theta) = \Phi_0\rho^n , \tag{15}$$

where $\varepsilon_h = \varepsilon_a\alpha\rho^2$, ε_a is the inverse aspect ratio, $\varepsilon_a = a / R_0$ (a is the plasma radius and R_0 is the major radius) and α is given approximately by

$$\alpha \simeq (M\iota_0 / 4)^{1/2}M\varepsilon_a . \tag{16}$$

The ripple form, Eq.(14) contains the l, $l + 1$ ($\delta_h^{(+1)}$) and $l - 1$ ($\delta_h^{(-1)}$) components of helical ripple. This expression, Eq.(14) is discussed in [5,6]. We note that Eq.(14) reduces to the σ - configuration, $B_l = \bar{B}_0\varepsilon_h(1 + \sigma\cos\theta)$, which are used for the transport optimization [7], when $\delta_h^{(\pm1)} = -2\sigma\alpha$. The modulating envelope

$$1 + [(\delta_h^{(-1)} + \delta_h^{(+1)}\rho^2) / \alpha\rho]\cos\theta$$

localizes the ripple to the interior (exterior) of the torus, for $\delta_h^{(-1)}, \delta_h^{(+1)} \geq 0$ (≤ 0) . The rotational transform associated with ψ_p in Eq.(5) is assumed to be

$$\iota(\psi) = -\frac{d\psi_p}{d\psi} = \iota_0 + (\iota_e - \iota_0)\rho^2 , \tag{17}$$

where ι_0 and ι_e are the values of $\iota(\psi)$ at the location of magnetic axis and at the plasma edge, respectively. Equations (16) and (17) give ψ_p as

$$2\pi\psi_p = -(2\alpha^2 / M^3)\bar{B}_0R_0\rho^2[1 + (\iota_e - \iota_0)\rho^2 / (2\iota_0)] . \tag{18}$$

Ⅱ. ANALYSIS OF LOSS REGION

The constant - J_r surfaces describe drift surfaces of trapped particles in helical ripples. On the other hand, the constant - $J_\pm$ surfaces give drift surfaces for passing and blocked particles.

We here explain the analysis of drift orbit loss regions in configuration space by using the adiabatic invariants, (5) ~ (7) . Particle motions in toroidal helical systems are generally characterized by drift surfaces defined by the constant- J_r and constant- $J_\pm$ surfaces, and the transition between these two surfaces. To simplify the analysis, we introduce the quantity λ_0 by

$$\lambda_0 = \frac{\mu B_0}{E} , \tag{19}$$

which is related to the pitch angle in velocity space. Then, k^2 can be expressed as $k^2 = k^2 (\rho, \theta ; \lambda_0)$. The $k^2 = 1$ locus for a fixed value of λ_0 is called a transition curve in (ρ, θ) plane. The interior of the transition curve is $k^2 \geq 1$ and drift surfaces belong to the passing and blocked particles. Outside the transition curve, drift surfaces are characterized by localized particles.

In helical configurations, the loss region caused by the trapped particles is formed both outside and inside the torus. Generally, the loss region outside the torus is bigger than inside the torus because the drift orbit of trapped particle is shifted inside the torus due to the toroidal effect. We here analyze the loss region outside the torus although the loss region inside the torus can also be studied in the same way. We assume that all particles start from a position outside the torus (ρ_0, π) , and a circular limiter is located at $\rho = \rho_s$. We consider the following three cases associ-

ated with the boundary of particle loss.

(a) When ρ_0 is outside the transition curve, the drift surface is determind by J_r = constant. If the drift surfaces of localized particles hit the limiter at (ρ_s , 0) , these particles are defined as lost particles. This condition gives a marginal value for λ_0 or a corresponding pitch angle in velocity space. From the condition J_r (ρ_0 , π ; λ_0) = J_r (ρ_s, 0 ; λ_0), i.e.,

$$\varepsilon_{10}^{-1/2}\left[(1 + \gamma_0 k_0^2)\Pi(\gamma_0 k_0^2 ; k_0^2) - K(k_0^2)\right]$$

$$= \varepsilon_{1s}^{-1/2}\left[(1 + \gamma_s k_s^2)\Pi(\gamma_s k_s^2 ; k_s^2) - K(k_s^2)\right], \tag{20}$$

with the abbreviations of

$$k_0^2 = k^2(\rho_0, \pi ; \lambda_0), \quad k_s^2 = k^2(\rho_s, 0 ; \lambda_0),$$

$$\gamma_0 = \gamma(\rho_0, \pi), \qquad \gamma_s = \gamma(\rho_s, 0),$$

$$\varepsilon_{10} = \varepsilon_1(\rho_0, \pi), \qquad \varepsilon_{1s} = \varepsilon_1(\rho_s, 0),$$

we obtain the solution, $\lambda_0 = \lambda_a(\rho_0)$ with other parameters fixed. Localized particles with $\lambda_0 > \lambda_a$ are confined within $\rho < \rho_s$ and those with $\lambda_0 < \lambda_a$ go outside $\rho = \rho_s$.

(b) Blocked and passing particles exist inside the transition curve. We here study the particle loss associated with the transition process from a blocked particle with $\tilde{\sigma} = \pm$ starting from (ρ_0, π) to a localized particle. The confinement of blocked particles depends on whether the localized particles after the transition can be confined or not. We consider a case that the blocked particle starting from (ρ_0, π) moves along $J_\pm$ = constant path, and crosses the transition curve at (ρ_T, θ_T) where $k^2 = 1$, and it comes to the position of limiter (ρ_s, 0) along J_r = constant path. These particle motions are described by the relations

$$k^2(\rho_T, \theta_T ; \lambda_0) = 1, \tag{21}$$

$$J_{\tilde{\sigma}}(\rho_T,\ \theta_T\ ;\ \lambda_0) = J_{\tilde{\sigma}}(\rho_0,\ \pi\ ;\ \lambda_0), \tag{22}$$

$$J_r(\rho_s,\ 0\ ;\ \lambda_0) = J_r(\rho_T,\ \theta_T\ ;\ \lambda_0). \tag{23}$$

By eliminating ρ_T and θ_T in Eqs.(21), (22), and (23), we have the relations for $\lambda_0 = \lambda_{b+}\ (\rho_0)$ for $\tilde{\sigma} = +$ and $\lambda_0 = \lambda_{b-}\ (\rho_0)$ for $\tilde{\sigma} = -$, which determine the boundary of loss region caused by the blocked particles with $\tilde{\sigma} = \pm$. Blocked particles with $\lambda_0 < \lambda_{b+}$ and λ_{b-} are confined, and those with $\lambda_0 > \lambda_{b+}$ and λ_{b-} are lost.

(c) Here we give the boundary between the blocked particles and the passing particles. The radial position where the transition curve crosses the $\theta = 0$ plane is denoted by $\rho = \rho^*$. The boundary is given by the following relations ;

$$J_{\tilde{\sigma}}(\rho^*,\ 0\ ;\ \lambda_0) = J_{\tilde{\sigma}}(\rho_0,\ \pi\ ;\ \lambda_0)\ , \tag{24}$$

$$\lambda_0 = \left[1 - e\Phi_E(\rho^*)\ /\ E\right] \Big/ \left[\varepsilon_0(\rho^*,\ 0) + \varepsilon_1(\rho^*,\ 0)\right]\ . \tag{25}$$

From (24) and (25), we obtain $\lambda_0 = \lambda_{c+}(\rho_0)$ for $\tilde{\sigma} = +$ and $\lambda_0 = \lambda_{c-}(\rho_0)$ for $\tilde{\sigma} = -$. Particles with $\lambda_0 < \lambda_{c+}$ and λ_{c-} are passing particles and stay inside the transition curve.

When the solutions, λ_j ($j = a,\ b\pm$ and $c\pm$) are obtained, we can determine the corresponding pitch angle in velocity space at the initial position from

$$\sin^2\chi_0 = \frac{\lambda_0}{1 - e\Phi_E(\rho_0)\ /\ E}\left[\varepsilon_0(\rho_0,\ \pi) - \varepsilon_1(\rho_0,\ \pi)\cos\tilde{\varphi}\right]\ , \tag{26}$$

where we defined the pitch angle χ_0 at the starting point $(\rho_0,\ \theta_0 = \pi,\ \varphi_0)$ as

$$\sin^2\chi_0 = \mu B\ /\ (E - e\Phi_E)\ . \tag{27}$$

For a specific case of $\tilde{\varphi} = 0$, therefore, the loss boundary determined by localized particles with $\chi_0 = \pi\ /\ 2$ is given by

$$[\varepsilon_0(\rho_0,\ \pi)\ -\ \varepsilon_1(\rho_0,\ \pi)][1\ -\ e\Phi_E(\rho_s)\ /\ E]$$

$$=\ [\varepsilon_0(\rho_s,\ 0)\ -\ \varepsilon_1(\rho_s,\ 0)]\ [1\ -\ e\Phi_E(\rho_0)\ /\ E]\ . \qquad (28)$$

Consequently, we can determine the relationship between λ_j or χ_0 and ρ_0 , which describe the boundaries of loss region caused by localized, blocked and passing particles.

Ⅳ. RESULTS OF LOSS REGIONS

We now discuss the structure of loss region for several helical configurations. Parameters of these configurations are shown in Table 1, where the magnetic field strength for all cases is fixed to be *4T* and we use the parameters of existing machine for M = 12 (ATF)[8] and also use the machine parameters at the design stage [9] for M = 10 and 14.

We first analyze the loss region in configuration space for the system with M = 14 . The values of λ_j (j = a, $b\pm$ and $c\pm$) obtained from Eqs. (20) ~ (25) versus ρ_0 are plotted in Fig.1. The values of λ_0 corresponding to k_0^2 = 0 , k_0^2 = 1 , k_s^2 = 0 , and k_s^2 = 1 are also shown in this figure. The region surrounded by k_0^2 = 0 , k_0^2 = 1 and k_s^2 = 0 curves represents the existing region of localized particles. Here, we used the parameters ; E = 10keV , ρ_s = 1 , Φ_0 = 0 , $\delta_n^{(+1)}$ = $\delta_n^{(-1)}$ = 0 and φ_0 = 0 . The curve λ_a indicates the loss boundary caused by localized particles. It should be noted that the solution λ_a is independent of the sign of $\tilde{\sigma}$. The curves λ_{b+} and λ_{b-} yield the loss boundaries caused by blocked particles with $\tilde{\sigma}$ = ± , respectively. The boundaries between passing and blocked particles are shown

by λ_{c+} and λ_{c-} . The difference between these curves, λ_{b+} versus λ_{b-} and λ_{c+} versus λ_{c-} comes from the different shift of drift orbits for $\tilde{\sigma} = \pm$, and it gives an asymmetric structure of loss region around $v_{\parallel} = 0$ or $\chi_0 = \pi / 2$.

Particle loss diagram in pitch angle and major radius (χ_0, ρ) plane are shown in Fig.2 for $M = 10$ (broken line) , 12 (dotted line) and 14 (solid line) configurations. It turns out from these results that the loss region is sensitive to M - number because of the variation of the ratio between toroidal and helical ripples, $\varepsilon_t / \varepsilon_h$, and the configuration with large M is generally preferable for the reduction of particle loss. The loss boundary caused by localized particles with $\chi_0 = \pi / 2$ can easily be evaluated from Eq.(28) in case of $\varphi_0 = 0$. We denote this loss boundary by ρ_{LUB}. Also, we can evaluate numerically the lower limit of loss boundary (we represent ρ_{LLB} hereafter) , which is caused by the transition particles. As shown in Fig.2, we have these loss boundaries ;
$\rho_{LUB} = 0.2845 (M = 10)$, 0.4307 $(M = 12)$ and 0.5442 $(M = 14)$, and
$\rho_{LLB} = 0.0543$ $(M = 10)$, 0.1384 $(M = 12)$ and 0.2157 $(M = 14)$.

Generally, the loss region can be reduced by adding the side band components such as $\varepsilon_h^{l\pm1}$. These components are practically provided by the shift of magnetic axis due to vertical field, the pitch modulation of helical winding and so on. We study the effect of side band components on particle loss on the basis of a model of ripple modulation, Eq.(14) . Particle loss diagrams in χ_0–ρ plane are plotted in Fig.3 for $M = 14$ configurations with $\delta_h^{(+1)} = \delta_h^{(-1)} \equiv \delta_h^{(1)} = 0.0$ (a) , 0.1 (b) and 0.2 (c) . The other parameters used here are the same as the case of $M = 14$ in Fig.2 . The present results show that the positive ripple modulation ($\delta_h^{(+1)} > 0$ and $\delta_h^{(-1)} > 0$) has a good effect on the reduction of particle loss. Similar results have been discussed recently.[10]

We next study the effect of radial electric field on the particle confinement. Particle loss regions in χ_0–ρ plane are shown in Fig.4 for several values of electric potential Φ_0 in the $M = 14$ configuration. As for the potential profile is concerned, we assume a parabolic profile, $\Phi_E = \Phi_0\rho^2$ $(n = 2)$. The result for $\Phi_E = \Phi_0\rho^4$ $(n = 4)$ with $\Phi_0 = -2$KV is also shown by dotted line. It turns out that the case of $\Phi_E \sim \rho^4$ has an influence on the improvement of particle confinement more than the case of $\Phi_E \sim \rho^2$ does. Loss boundaries, ρ_{LUB} (closed circles) and ρ_{LLB} (open circles) in Φ_0–ρ plane are plotted in Fig.5. The analytical result for ρ_{LUB} calculated by Eq.(28) is shown by solid curve in this figure. The region below these curves represents the particle loss region. Negative potential leads the reduction of particle loss and the positive potential degradates the particle confinement in the outside of torus, when the ion motion is considered.[11] Degradation of the confinement for some value of positive potential is caused by a large shift of drift surface from magnetic surface. Generally, the particle confinement may be improved for a large potential regardless of its sign due to large poloidal rotation by $E \times B$ drift. For the configurations under consideration in this paper, the occurrence of helical resonance may enhance the particle losses.

V. NUMERICAL ANALYSIS BASED ON DRIFT EQUATIONS

In this section we study the loss regions in both configuration and velocity space by solving the guiding center drift equations. The normalized drift equations can be written in the magnetic coordinates (ψ, θ_0, χ)[14]

$$\frac{d\theta_0}{dt} = \frac{\partial\Phi}{\partial\psi} + (\mu + B\rho_{\parallel}^2)\ \frac{\partial B}{\partial\psi}, \tag{29}$$

$$\frac{d\psi}{dt} = -\frac{\partial \Phi}{\partial \theta_0} - (\mu + B\rho_{\parallel}^2)\ \frac{\partial B}{\partial \theta_0}, \tag{30}$$

$$\frac{d\chi}{dt} = B^2\rho_{\parallel}\ , \tag{31}$$

$$\frac{d\rho_{\parallel}}{dt} = -\frac{\partial \Phi}{\partial \chi} - (\mu + B\rho_{\parallel}^2)\ \frac{\partial B}{\partial \chi}, \tag{32}$$

with

$$B(\psi,\ \theta_0,\ \chi) = 1 - \varepsilon_a(2\psi)^{1/2}\cos\theta$$

$$- \Big[\{2\varepsilon_a\alpha\psi - (\delta_h^{(-1)} + 2\delta_h^{(+1)}\psi)\varepsilon_a(2\psi)^{1/2}\cos\theta\}^2$$

$$+ \{(\delta_h^{(-1)} - 2\delta_h^{(+1)}\psi)\varepsilon_a(2\psi)^{1/2}\sin\theta\}^2\Big]^{1/2}\cos\eta \tag{33}$$

where $\mu B = (1/2)mv_{\perp}^2$, $\rho_{\parallel} = v_{\parallel}(mc\ /\ eB)$, Φ is an electrostatic potential, and $\eta \equiv l\theta - M\varphi$, $\theta = \iota\varepsilon_a\chi + \theta_0$, $\iota = \iota_0 + 2(\iota_e - \iota_0)\psi$. All quantities in Eqs.(29) ~ (33) are normalized in the same manner of Ref.[14] .

We can evaluate the loss region by solving Eqs.(29) ~ (32). Typical results for loss regions in both configuration space and velocity space at the position of $\rho = 0.5$ are shown in Fig.6a and 6b for the case of $M = 14$. The same parameters as in Fig.2 are used in the calculations. Also, we assumed $\iota_e = \iota_0 = 0.58$ in Figs.6. The particles are initially distributed uniformly in the region of pitch angle 40° to 140° and in major radius $\rho = 0$ to 1 in the plane of toroidal angle $\pi\ /\ 14$, and are assumed to be lost when they touch the limiter ($\rho = \rho_s = 1$). Passing, localized and blocked - transition particles are classified in Figs.6 by open circle (O), star (⋆) and lozenge (◻) , respectively. Loss regions are also represented by the small mark of each particle (O, ⋆, ◻) . Therefore, we can easily understand what

kind of lost particle determines the boundaries of loss region. The results are in qualitative agreement with the results derived by J - invariant method.

Ⅵ. CONCLUSIONS

The spatial structure of loss region has been studied by the adiabatic invariant method for several device parameters. Also we have carried out the numerical calculations by solving the guiding center drift equations. Although the contribution of finite banana width to the boundaries of loss region is not taken into consideration in the adiabatic invariant method, a good agreement between these two results has been obtained qualitatively on the spatial structure of loss regions.

Effects of ripple modulation on particle loss have been studied on the basis of a model of ripple modulation, Eq.(14) . It turned out that the positive $\delta_h^{(\pm 1)}$ component has a good effect on particle confinement.

Effects of radial electric potential have also been discussed. Drift motion due to negative potential reduces a number of localized particles and consequently leads the improvement of particle confinement. For a positive potential, however, there is a possible particle loss caused by the resonances. The present analysis based on the simple magnetic field model can not be applied directly to a more realistic magnetic field, which includes the effects such as vertical field, quadrapole field, pitch modulation of helical winding. The analysis involving these effects awaits futher investigations.

ACKNOWLEDGEMENT

We would like to thank Dr. K. Hanatani for his useful discussions.

References

1) D.Dobrott and E.A. Frieman , Phys. Fluids 14, 349 (1971).

2) M. Wakatani, S. Kodama, M. Nakasuga and K. Hanatani , Nucl. Fusion 21, 175 (1981).

3) J.R. Cary, C.L. Hedrick and J.S. Tolliver , Phys. Fluids 31, 1586 (1988).

4) J. Todoroki , submitted to J. Phys. Soc. Japan

5) W.N.G. Hitchon , Nucl. Fusion 22, 1661 (1982).

6) M. Wakatani , Nucl. Fusion 23, 817 (1983).

7) H.E. Mynick, T.K. Chu and A.H. Boozer , Phys. Rev. Lett. 48, 322 (1982).

8) J.F. Lyon, B.A. Carreras, K.K. Chipley, et al. , Fusion Technol. 10, 179 (1986)

9) J. Todoroki, T. Kamimura, H. Sanuki, T. Amano, T. Hayashi, K. Suzuki, T. Sato, K. Hanatani, M. Wakatani and A. Iiyoshi, in 12th IAEA Int. Conf. on Plasma Physics and Controlled Nuclear Fusion Research (Nice, 1988) paper IAEA-CN-50 / C-V-4-2.

10) A. Kato and M. Wakatani , J. Phys. Soc. Japan 58, 2423 (1989).

11) R.H. Fowler, J.A. Rome and J.F. Lyon, Phys. Fluids 28, 338 (1985).

12) K. Hanatani, F.P. Penningsfeld and H. Nobig, Proc. International Stellarator / Heliotron Workshop (IAEA Technical Committee Meeting), Kyoto, Japan, 1986, Vol.2, p.444.

13) K. Hanatani et al., Proc. 14th European Conf. Controlled Fusion and Plasma Physics, Madrid, Spain, 1987, Vol. 11D, Part 1, p.396, European

Physical Society.

14) A.H. Boozer and G. Kuo-Petravic, Phys. Fluids 24, 854 (1981)

Table Caption

Table 1. Machine parameters used in numerical calculations

Figure Captions

Fig.1 Values of λ_j charactering loss boundaries associated with localized particles (λ_a), blocked - localized transition particles (λ_{b+} for $\tilde{\sigma} = +$ and λ_{b-} for $\tilde{\sigma} = -$), and passing - blocked transition (λ_{c+} for $\tilde{\sigma} = +$ and λ_{c-} for $\tilde{\sigma} = -$) are shown as a function of ρ . Boundaries of $k_0^2 = 1$, $k_0^2 = 0$, $k_s^2 = 1$, and $k_s^2 = 0$ are also plotted. Parameters for $M = 14$ configuration are used.

Fig.2 Particle loss diagram in pitch angle and normalized major radius ($\chi_0 - \rho$) plane is shown for $M = 10$, (broken line), 12 (dotted line) and 14 (solid line) configurations.

Fig.3 Effect of ripple modulation on particle loss. Results for $M = 14$ configuration with $\delta_h^{(\pm 1)} = 0.0$ (a), 0.1 (b) and 0.2 (c) are plotted. Boundaries for $k_0^2 = 1$ are also shown by small dotted lines.

Fig.4 Particle loss diagram in χ_0-ρ plane in $M = 14$ configuration is shown for several values of Φ_0 , where $\Phi_E = \Phi_0\rho^2$ is used. Results for $\Phi_E = \Phi_0\rho^4$ with $\Phi_0 = -2$KV is also plotted by dotted line. (a) $\Phi_0 = 0.0$, (b) $\Phi_0 = -2$KV , (c) $\Phi_0 = -4$KV . The boundary for $k_0^2 = 1$ is also shown by small dotted line.

Fig.5 Loss boundaries corresponding Fig.4, ρ_{LUB} (closed circles) and ρ_{LLB}

(open circles) are shown in Φ_0-ρ plane. Analytical results for ρ_{LUB} given by Eq.(28) is shown by solid curve.

Fig.6 Numerical results of particle loss region in configuration space (Fig.6a) and velocity space at ρ = 0.5 (Fig.6b) , which are obtaind by solving drift equations. Parameters of M = 14 configuration are used, but $\iota_e = \iota_0 = 0.58$ and $\delta_n^{(\pm 1)} = 0$ are assumed.

M	B(T)	R(m)	a_p(m)	ε_t	ε_h	iota(0)	iota(a_p)
14	4	5.0	0.55	0.110	0.24	0.58	2.0
12	4	3.5	0.5	0.143	0.25	0.35	0.95
10	4	4.0	0.5	0.125	0.17	0.5	0.9

Table 1

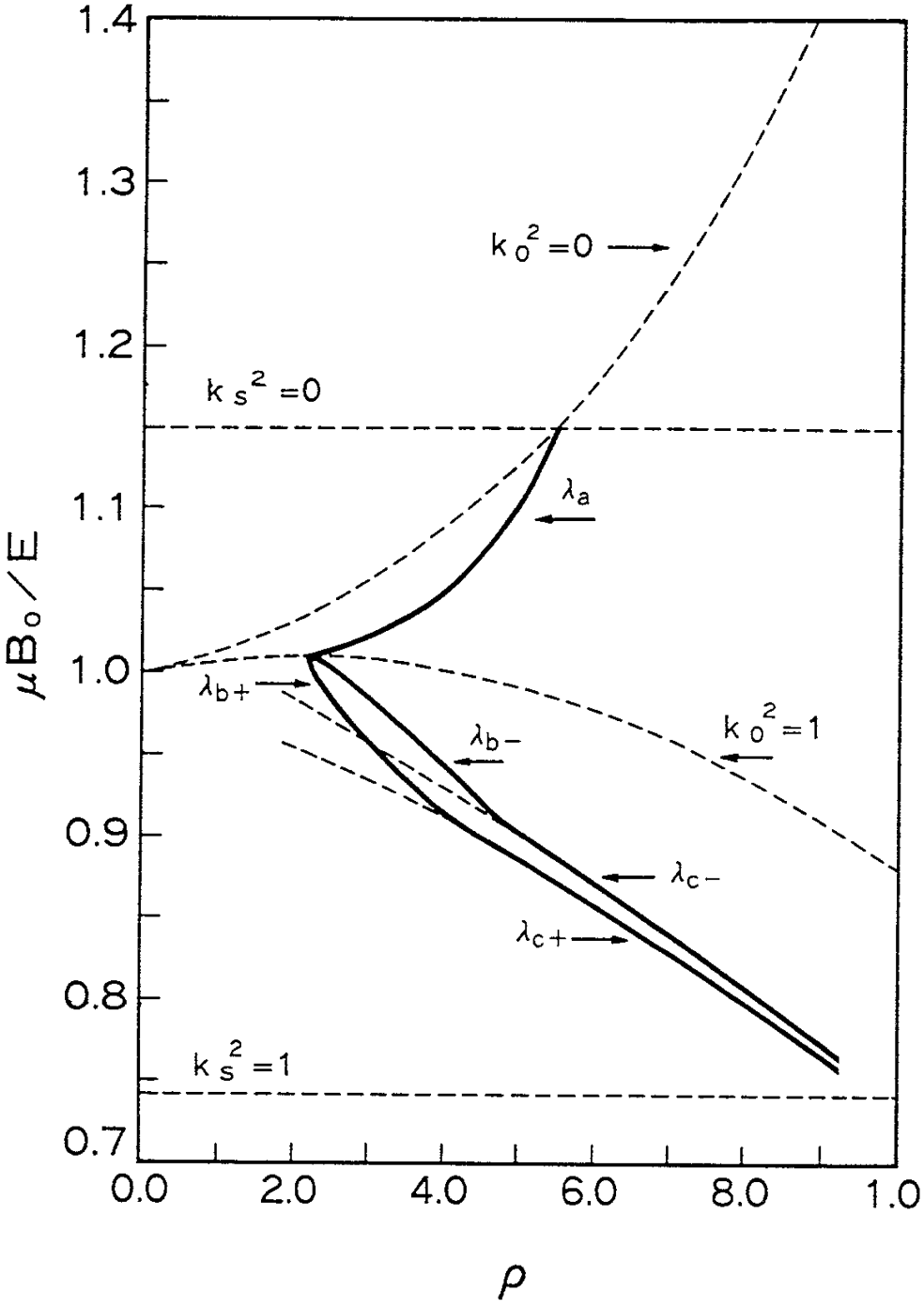
1.4
1.3
1.2
1.1
1.0
0.9
0.8
0.7
μB₀/E
0.0
2.0
4.0
6.0
8.0
1.0
ρ
k₀²=0
kₛ²=0
λa
λb+
λb−
k₀²=1
λc−
λc+
kₛ²=1

Fig.1

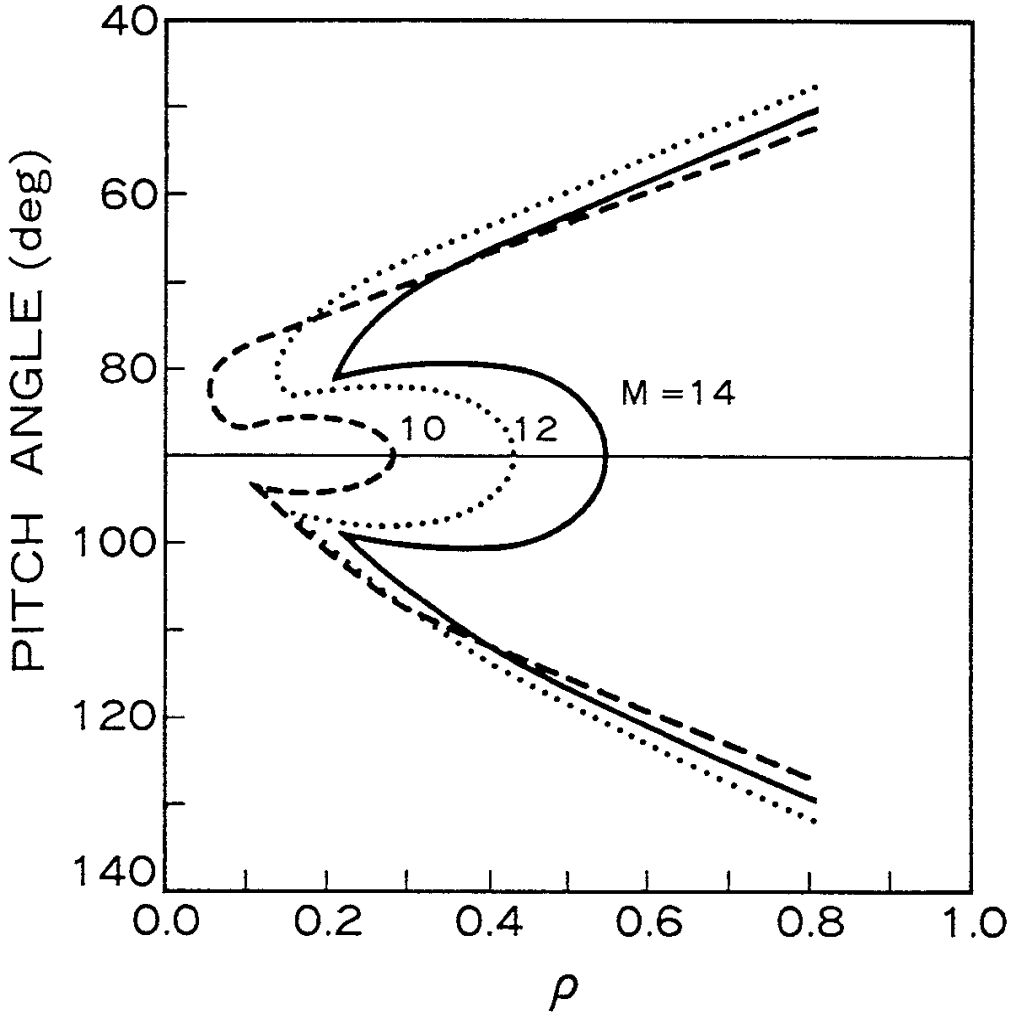

Fig.2

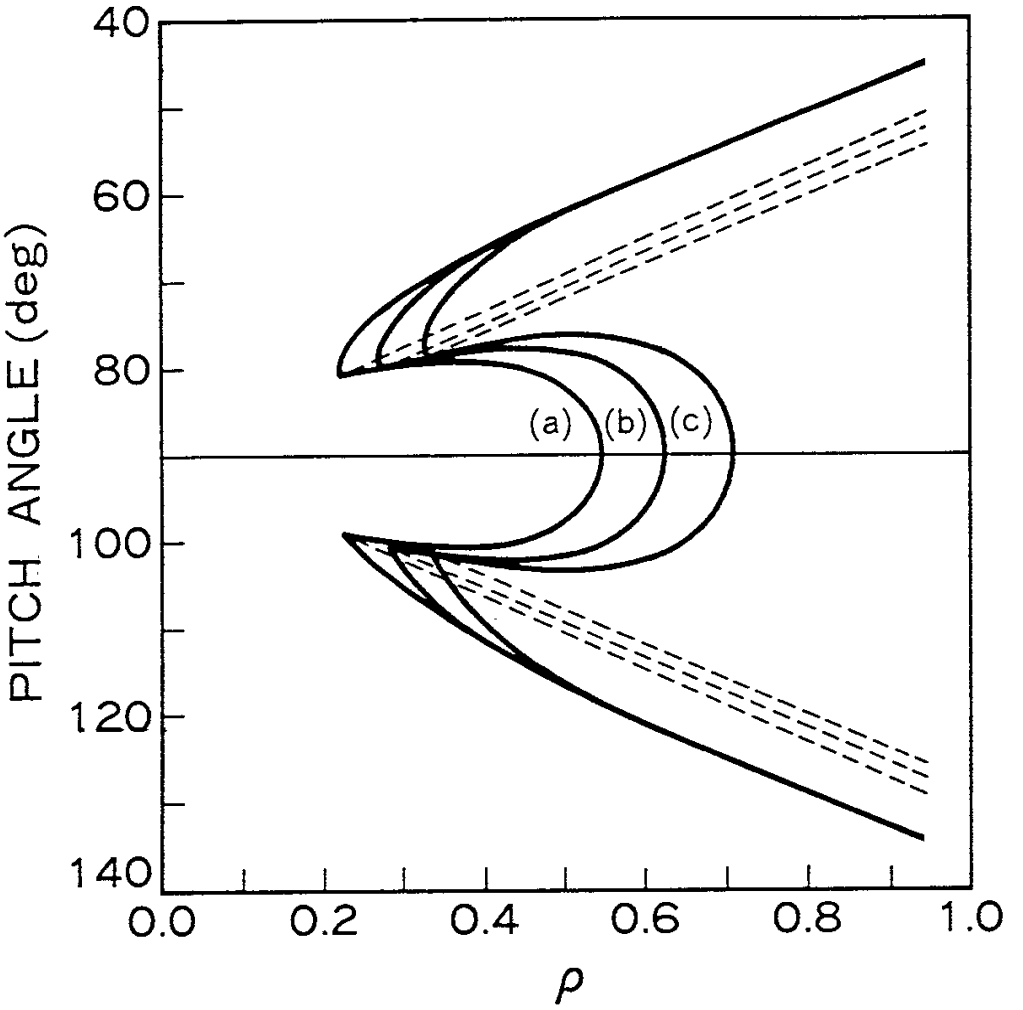

Fig.3

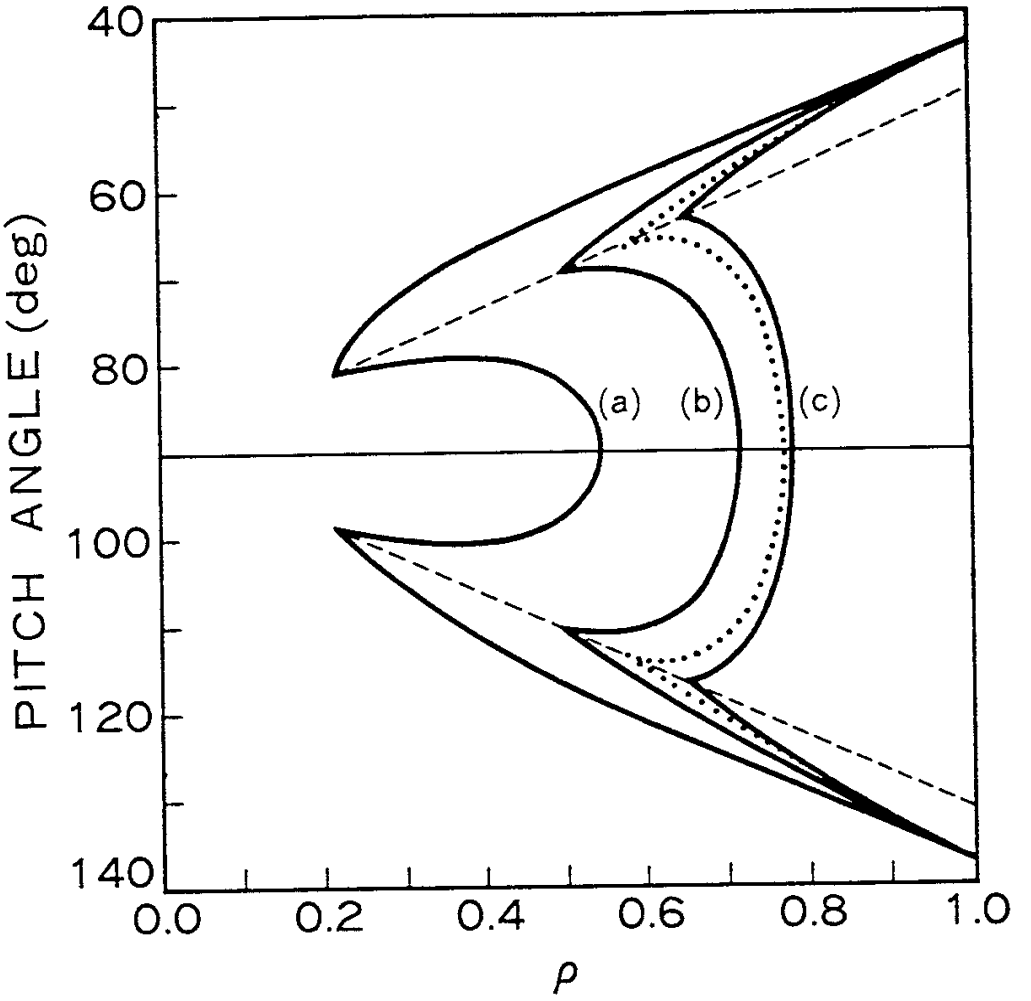

Fig.4

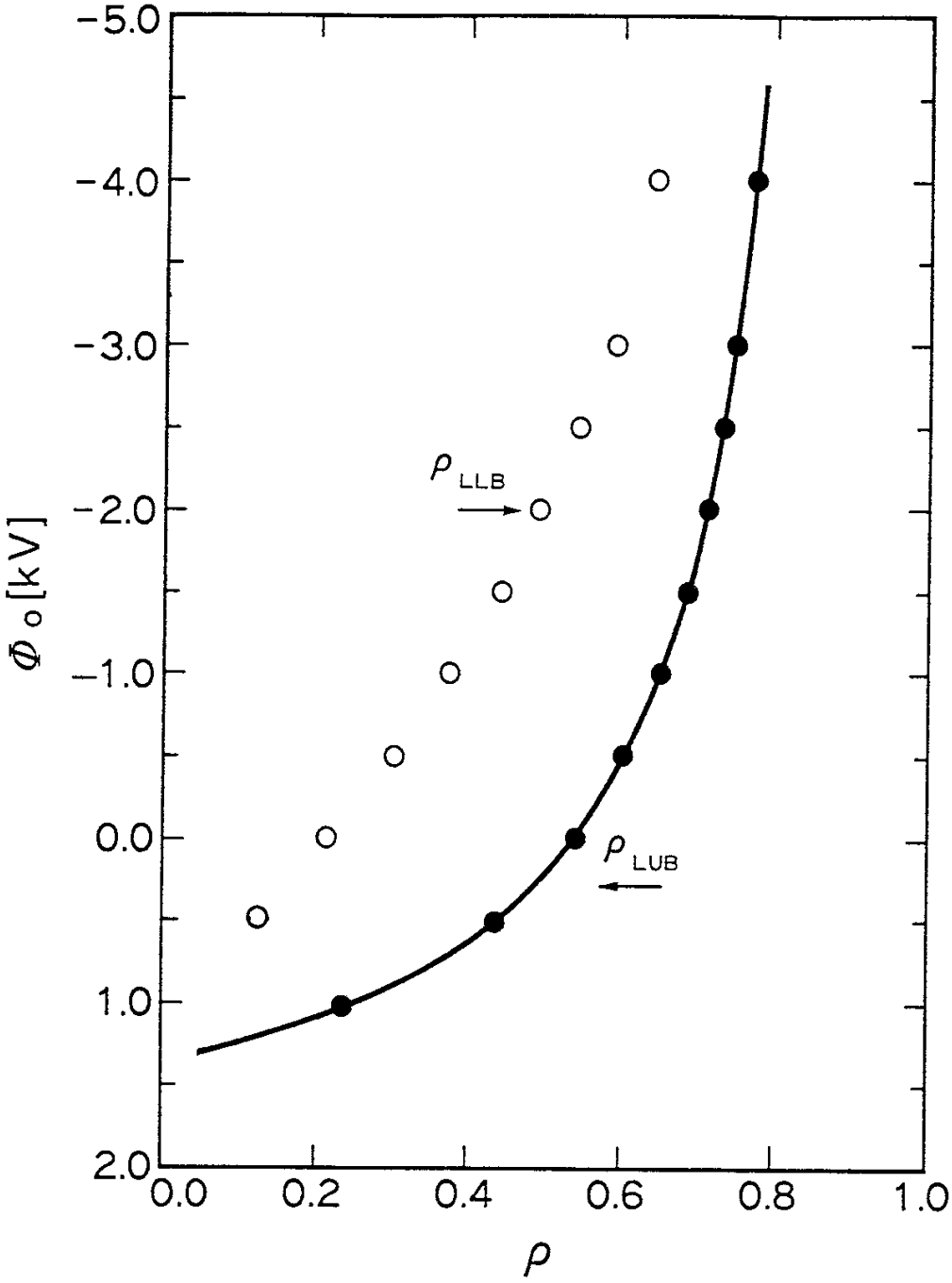

Fig.5

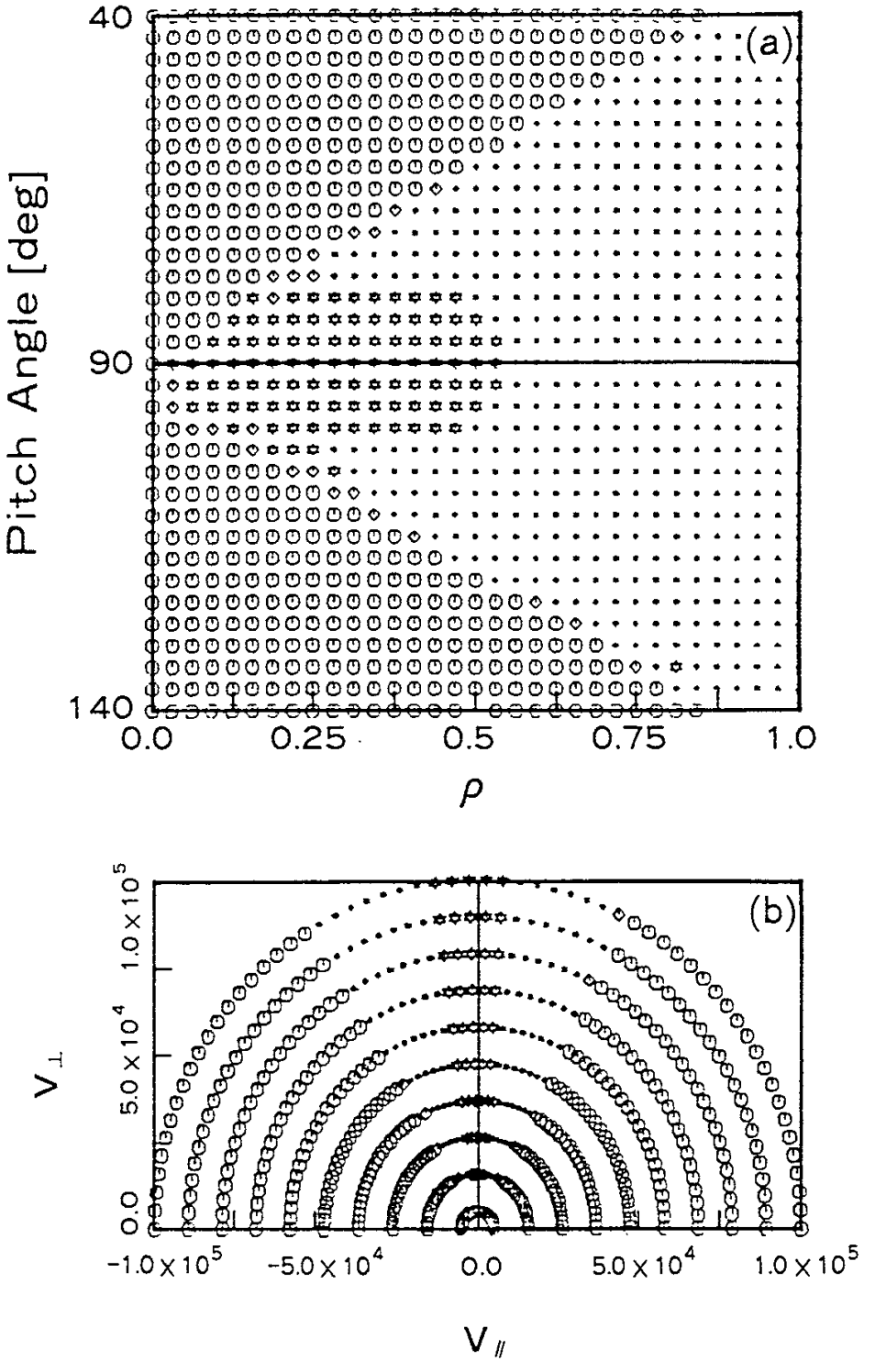
(a)
Pitch Angle [deg]
40
90
140
0.0
0.25
0.5
0.75
1.0
ρ
(b)
$V_\perp$
1.0×10^5
5.0×10^4
0.0
-1.0×10^5
-5.0×10^4
5.0×10^4
1.0×10^5
$V_{//}$

Fig.6